Bioprocess Engineering
2023; 7(1): 10-31
http://www.sciencepublishinggroup.com/j/be
doi: 10.11648/j.be.20230701.12
ISSN: 2578-8698 (Print); ISSN: 2578-8701 (Online)

Evaluation of Thin Layer Models for Simulating Drying Kinetics of Black Nightshade Seeds in a Solar-Exhaust Gas Greenhouse Dryer

George Onyango Orido[1, 2, *], Erick Kiplangat Ronoh[1], Patrick Ochuodho Ajwang[1], Benson Baari Gathitu[1]

[1]Agricultural and Biosystems Engineering Department, Jomo Kenyatta University of Agriculture and Technology, Nairobi, Kenya
[2]Agricultural Engineering Department, Egerton University, Nakuru, Kenya

Email address:

george.orido@egerton.ac.ke (George Onyango Orido), ronoh@jkuat.ac.ke (Erick Kiplangat Ronoh), ajwang@agr.jkuat.ac.ke (Patrick Ochuodho Ajwang), bbgathitu@jkuat.ac.ke (Benson Baari Gathitu)

[*]Corresponding author

To cite this article:

George Onyango Orido, Erick Kiplangat Ronoh, Patrick Ochuodho Ajwang, Benson Baari Gathitu. Evaluation of Thin Layer Models for Simulating Drying Kinetics of Black Nightshade Seeds in a Solar-Exhaust Gas Greenhouse Dryer. *Bioprocess Engineering*. Vol. 7, No. 1, 2023, pp. 10-31. doi: 10.11648/j.be.20230701.12

Received: April 10, 2023; **Accepted**: April 25, 2023; **Published**: May 10, 2023

Abstract: The current study aimed to use, besides solar, waste heat from exhaust gas of a diesel engine operated for milling of grain, to dry black nightshade seeds. Assessment of thin layer models for simulating drying kinetics of black nightshade seeds was performed in a solar-exhaust gas greenhouse dryer operated on solar; solar-exhaust gas; and exhaust gas modes. In solar mode, seeds took 11 hours to reach a final moisture content of 7.13% (db) from an initial one of 89.34% (db). In solar-exhaust gas mode seeds were dried from an initial moisture content of 92.57% (db) to a final one of 6.07% (db) in 10 hours. In exhaust gas mode it took 14 hours to dry black nightshade seeds from an initial moisture content of 88.84% (db) to a final one of 9.42% (db). Newton, Page, Logarithmic, and Henderson and Pabis thin layer drying models were fitted to experimental data and the best model was selected based on low root mean squared error (RMSE) and interpretation of residual plots. To best explain the prediction of thin layer drying of black nightshade seeds, based on the lowest value of RMSE, Page model was found suitable for solar mode with RMSE of 0.01147206, Logarithmic model was found suitable for both solar-exhaust gas and exhaust gas modes of drying with RMSE of 0.0172098 and 0.02315325 respectively. In conclusion, the thin layer modeling approach can be used to provide design data for a solar-exhaust gas greenhouse dryer.

Keywords: Solar-Exhaust Gas Greenhouse Dryer, Thin Layer Drying, Page Model, Logarithmic Model, Black Nightshade Seeds

1. Introduction

Black nightshade (*solanum villosum*) is a worldwide leafy herb and vegetable of arable land, gardens, rubbish tips, soil rich in nitrogen in moderately light and warm situations which occur from sea to montane levels [1]. Black nightshade is also commonly known as the orange-fruit nightshade and is widely distributed in many parts of the world. The species is reported to be common in northern parts of Africa where it could well be native. It is widely distributed at altitudes of 792-3048 m above the sea level in Cameroon, Ethiopia, Kenya, Somalia, South Africa, Tanzania, and Uganda. The vernacular names of black nightshade in Kenya are: mnavu (Swahili), amanagu (Kisii), namasaka (Luhya), Kitulu (Kamba), ndunda (Taita), sochot (Keiyo), sujet (Kinandi), isusa (Maragoli), ol'momoit (Masai), soiyot (Kipsigis), manago (Kikuyu), and osuga (Luo). Its propagation is through seeds which have a long shelf life depending on the storage conditions and the seeds moisture content—the recommended being 5 ± 1% [2]. Black nightshade seeds are planted in nurseries and the germination time is usually 5-7 days. The seeds sown will be in the nursery for one month from the time of sowing to transplanting. Black

nightshade vegetable takes about 5 weeks from transplanting for the first harvest of the leafy vegetable to take place [3].

According to Edmonds and Chweya [1], black nightshade is an Ayurvedic herb with multiple medicinal properties. Ethnobotanical uses of black nightshade reported by the authors both in literature and herbarium material are based on beneficial properties such as: a source of food, nutritional value, medicinal value, a source of fodder and browse, commercial value, and rural and urban economic value. Throughout the world, boiled or stewed leaves and tender shoots of black nightshade are widely used as vegetables—a food source during famine—and in soups and sauces. In the respective geographical ranges in Africa, the vegetable crop is used as port-herbs and the vegetative parts are boiled in water, which is discarded and replaced several times, or replaced with milk to add taste and flavor to the diet and make it delicious. Schippers [3] has, however, reported that vitamins and other micro-nutrients are unfortunately thrown away with the discarded water, thereby reducing the nutritious value of black nightshade. In Kenya, black nightshade is used in both rural and urban areas with a good demand in Nairobi which can hardly be met by farmers from the surrounding areas such as Embu. Farmers from as far away as Kisii, South Nyanza, and Western Kenya have been reported to have made arrangements to transport their black nightshade produce to the capital city [3]. In the rural areas, the consumption of green leafy black nightshade is believed to result in the birth of children with dark eyes and smooth skin, therefore, the boiled leaves of the vegetable are recommended for pregnant women [1]. In addition, pregnant women who eat this vegetable are believed to recuperate well after delivery. In parts of Western Kenya, the orange ripe berries of black nightshade are frequently eaten raw as fruits. Edmonds and Chweya [1] reported that several studies had been conducted to investigate the nutritive value of black nightshade. The authors summarized the nutritive value of the vegetable crop under nutrient per 100-g of edible portion and range of values as: water (83-91%), crude protein (2.8-5.8 g), crude fibre (0.6-1.4 g), fat (0.8 g), carbohydrates (3.3-5.0 g), calories (38 kcal), ethereal extract (38-44 g), iron (1.0-4.2 mg), calcium (99-442 mg), phosphorous (75 mg), beta-carotene (1.7-11.6 mg), ascorbic acid (20-158 mg), oxalate (58.8-98.5 mg), nitrate-N (29-400 mg), and total phenolics (68.3-73.4 mg).

The bruised fresh leaves of black nightshade are used externally to ease pain and reduce inflammation when applied to burns, used for ringworms, gout, and earache. In Western Kenya, black nightshade's reputation as a good gargle and mouthwash has been reported [3, 1]. The raw fruits of the vegetable crop when chewed and swallowed will treat stomach ulcers, general abdominal pain, and stomach-ache. Children who have developed crooked teeth may have infusions of leaves and seeds rubbed onto their gums to ease pain. Pounded leaves and fruits form an infusion used against tonsilitis, muscular and joint pains associated with malarial fever and arthritis. Cattle, sheep, and goats in Kenya are known to feed on black nightshade vegetable as fodder and browse. Macerated leaves and berries produce a dye and ink source used to colour sisal and baskets. This commercial value is realized because black nightshade is a useful source of colorants, the pigment is present in high concentration, it is vigorous and easy to grow. Most women from Western Kenya have benefitted from the sale of the vegetable crop in both rural and urban markets [3].

Drying is among the easiest and more affordable ways of preserving black nightshade seeds through moisture content reduction by application of heat to the seeds. The abundance of solar energy has made greenhouse solar drying a possibility in dryers designed for agricultural produce. However, for prolonged drying when solar radiation is low and at nighttime a solution to supplement greenhouse solar drying—use of heat energy from exhaust gas—was provided in the current study with the achieved objective of drying time reduction when a combination of solar and exhaust gas use was studied. In this work, drying characteristics of black nightshade seeds were qualitatively studied based on the concept of exhaust gas heat recovery from a diesel engine used in a solar-exhaust gas greenhouse dryer. Kiburi *et al*. [4] developed a solar-biomass hybrid greenhouse dryer consisting of a biomass stove and double duct heat exchanger when drying banana slices. The authors concluded with a recommendation of nighttime drying using biomass followed by daytime drying using appropriate energy mode—solar or a combination of solar-biomass—to save on drying time. In the present work, the biomass unit developed by Kiburi *et al*. [4] was replaced with a hybrid-recuperative heat exchanger for diesel engine generated exhaust gas to supplement the heat energy requirements of the dryer at nighttime and during daytime when solar radiation was below average. Ronoh *et al*. [5] have reported the importance of thin layer drying models as tools used to describe drying kinetics of agricultural produce. Improvement of drying was reported by the authors as an advantage that positively affect the design of efficient dryers thus preventing the sole reliance on experimental drying practices without considerations of the mathematics of drying kinetics. Thin layer drying of black nightshade seeds was performed in the present work to determine the drying kinetics of the product—involving simultaneous heat and mass transfer operations—with an aspect of mathematical modeling of the drying process. According to Chowdhury *et al*. [6] and Hii *et al*. [7] thin layer drying models fall into three categories: theoretical, semi-theoretical, and empirical. Newton; Page; Logarithmic; and Henderson and Pabis models used in this study are classified under semi-theoretical models which offer a compromise between theory and ease of application. Ronoh *et al*. [5] have argued that food drying kinetics is a complex phenomenon requiring simplicity for drying behaviour prediction and optimization of parameters. On prediction accuracy of thin layer drying models, the authors reported that the selection and appropriateness of a model in describing the drying behaviour of an agricultural produce may not depend on the number of constants or coefficients but on statistical indicators as supported by Onwude *et al*. [8].

Moreover, limited studies have been conducted on thin

layer drying of black nightshade seeds. Justifiably, there is need to study the effect of drying modes on quality characteristics of the seeds because drying is an energy intensive process requiring harvested seeds with an initial moisture content of 88-93% to be dried to an equilibrium moisture content (EMC) of 5±1% [2] by using energy in a solar-exhaust gas greenhouse dryer—an alternative for Kenyan farmers—rather than open sun drying. The drying technique used in the current work was fast on solar-exhaust gas mode, protected black nightshade seeds from exposure to the environment and prevented contamination due to dust and insects. Black nightshade seeds are small in size and can easily be blown away by the actions of wind if not dried in a protected environment—solar-exhaust gas greenhouse dryer—as has been performed in this study. Heat energy from a diesel engine generated exhaust gas was a supplemental source during nighttime phase of drying and daytime when solar radiation was low. Exposure of black nightshade seeds to full sun should be avoided, as this can cause overheating, killing the embryos, especially in humid climates.

The reasons given on the introduction section of this study justifies why the present work was chosen. This work was done to promote the conservation of black nightshade crop through seeds drying to recommended conditions to improve germination and subsequently to preserve the biodiversity of this beneficial vegetable crop—black nightshade has been reported to have larvicidal activity against *stegomyia aegypti*, a common vector of dengue fever—according to Chowdhury *et al*. [9]. The previous study concluded that *solanum villosum* offers promise as a potential bio control agent against *stegomyia aegypti* particularly in its markedly larvicidal effect. The use of black nightshade extract or isolated bioactive phytochemical has been recommended in stagnant water bodies for the control of mosquitoes which act as communicable diseases' vectors [9].

2. Materials and Methods

2.1. Description of Study Site

Field experiments were set up at the Department of Agricultural and Biosystems Engineering, Jomo Kenyatta University of Agriculture and Technology (JKUAT), Kenya. The latitude and longitude angles of the University are $1^{\circ}5'20.8''$S and $37^{\circ}0'30''$E, while the altitude is 1527 m above the sea level. The mean annual temperature is 19.85°C with a mean annual maximum temperature of 24.91°C and a mean annual minimum temperature of 14.79°C. The relative humidities range from 15-80%. The climate for the study site is considered warm and temperate with an annual bimodal rainfall of 1014 mm characterized by cold rainy seasons occurring from April to August and October to December each year.

2.2. Experimental Setup

The solar-exhaust gas greenhouse dryer used in this study is shown in Figure 1 (outside view) and Figure 2 (inside view). The measurements of the dryer were 8 m long, 4 m wide, and 2.6 m high. The dryer which was glazed with an ultraviolet stabilized polythene film (0.2 mm in thickness) was of a standard peak even span positioned in an east-west orientation to make full use of the available yearly solar energy. The installation based on the east-west orientation has been reported by Ronoh *et al*. [5] as the preferred longer axis orientation for latitudes less than 40°. The floor of the dryer was painted black, acted as a heat sink, and increased the conversion of light into heat. Four drying trays, two on the right and two on the left were fabricated inside the dryer to measure 6 m long by 1 m wide with a spacing of 0.3 m between the two levels of drying. Food-grade plastic mesh screen (green in colour) held the drying products in position during the experiment. Samples of freshly harvested black nightshade berries shown in Figure 3 were collected from Western Kenya. Black nightshade seeds were extracted from the berries by a fermentation process [10, 3, 1] where the seeds with the pulp were left to ferment for three days. The seeds were then separated, thoroughly washed with water, and dried in the solar-exhaust gas greenhouse dryer. The seeds were evenly spread in thin layers on the drying trays as shown in Figure 4.

Figure 1. *Outside view of the solar-exhaust gas greenhouse dryer.*

Figure 2. *Inside view of the solar-exhaust gas greenhouse dryer.*

Figure 3. *Freshly harvested black nightshade berries.*

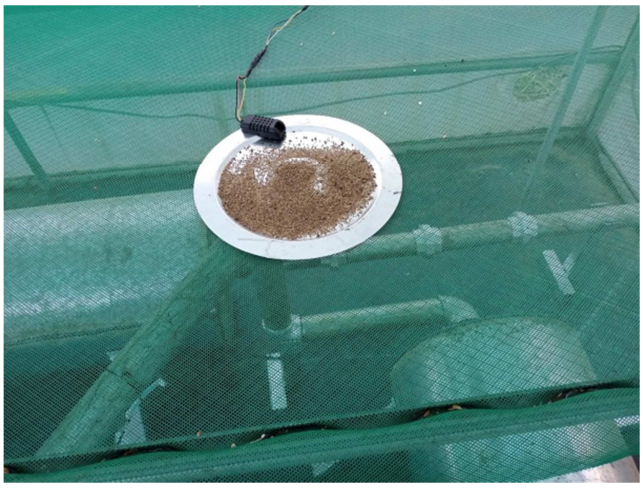

Figure 4. *Thin layer drying of black nightshade seeds on a drying tray.*

2.3. Instrumentation and Data Acquisition

To study the variation of temperature and relative humidity profiles inside and outside the solar-exhaust gas greenhouse dryer, twenty-six (AM2301A, China) temperature and relative humidity composite sensors with calibrated digital signal output were used. The sensors performance based on temperature characteristics were: resolution ratio of 0.1°C, accuracy of $\pm$0.5°C, measuring range of -40-80°C and repeatability of 0.2°C. Based on humidity characteristics, the sensors performance were: resolution of 0.1%, extended measuring range with a minimum of 0% and a maximum of 99.9%, accuracy of $\pm$0.3%, repeatability of $\pm$1%, and hysterisis of $\pm$0.3%. Twenty-four of the sensors were placed at the desired locations inside the dryer while one RH sensor and another temperature sensor were placed outside the solar-exhaust gas greenhouse dryer. Surface temperatures of connectors and tubes of the hybrid recuperative heat exchanger were measured using twelve (DS18B20, China) programmable resolution 1-wire digital thermometers with operating temperature range of -55°C to +125°C ($\pm$0.1). With reference to the solar-exhaust gas greenhouse dryer, inside and outside radiations were measured using two (MAX44009, China) ambient light sensors with digital outputs ideal for applications and operations in the dryer. The sensors (AM2301A, China), (DS18B20, China), and (MAX44009, China) were programmed to record data in a microcontroller (ATmega2560, Italy). The Arduino Mega microcontroller was equipped with a 2 GB microSD card for data storage of the drying experiments conducted between July 2022 and January 2023—the ideal period to perform experiments when the weather conditions were most suitable for solar, solar-exhaust gas, and exhaust gas modes. Mass of black nightshade seeds was recorded after one hour interval—until no further change in mass occurred—using a strain gauge based digital weighing machine with a precision of $\pm$0.01 g.

2.4. Drying Characteristics of Black Nightshade Seeds

The initial moisture content was determined according to Feldsine *et al*. [11] on AOAC method of analysis. 50 g of black nightshade seeds were placed in a moisture dish and both weights were taken. The seeds sample and moisture dish were placed in an oven and temperatures set at 105°C. The samples were removed and placed in a desiccator. The final mass was obtained after cooling. A constant mass was measured and recorded. Moisture content (% db) at any given drying time t (hours) was obtained using (1).

$$M = \frac{m_i - m_t}{m_t} \times 100 \quad (1)$$

In (1), M is moisture content in (% db); m_i is initial mass of sample (g); and m_t is dried mass of sample (g) at time t (hours). Ronoh *et al*. [5] and Uluko *et al*. [12] have reported that the relationship between drying time and moisture content is based on Newton model of thin layer drying for the material under varying relative humidity like in a solar-exhaust gas greenhouse drying. The instantaneous drying rate of black nightshade seeds was computed using (2) where DR is the drying rate (g/g/h), Δm is change in mass (g), Δt is change in time (h), m_{i-1} is the sample mass (g) preceding a given instantaneous sample mass, m_i (g), t_{i-1} is the drying time (h) preceding a given instantaneous drying time, t_i (h), and m_d is the final mass (g) of dried sample.

$$DR = \frac{\Delta m}{\Delta t} = \frac{m_{i-1} - m_i}{m_d(t_{i-1} - t_i)} \quad (2)$$

The moisture ratio at different drying time was computed using (3) from the data for moisture content of black nightshade seeds. Equation (3) is based on the theory of thin layer drying and MR is moisture ratio; M_t is the moisture content (% db) at time t in hours; M_e is equilibrium moisture content (%), M_i is initial moisture content (% db).

$$MR = \frac{M_t - M_e}{M_i - M_e} \quad (3)$$

Simulation of the drying process of black nightshade seeds in a solar-exhaust gas greenhouse dryer was done by the application of thin layer drying models described in Table 1. In Table 1, MR is moisture ratio; a and n are drying coefficients specific to each model; k is a drying constant (h^{-1}); and t is drying time (h).

Table 1. *Thin layer drying models used to describe drying kinetics of black nightshade seeds.*

Model	Equation	Citations
Newton	$MR = exp(-kt)$	Kaya *et al.* [13]
Page	$MR = exp(-kt^n)$	Abalone *et al.* [14]
Logarithmic	$MR = a \cdot exp(-kt) + c$	Goyal *et al.* [15]
Henderson and Pabis	$MR = a \cdot exp(-kt)$	Jayas *et al.* [16]

2.5. Models Validation

Models validation was a necessary step to examine the thin layer drying models used in this work. The initial scrutiny involved studying the values predicted by the model with those observed as experimental data. First, the performance of the models was measured in terms of root mean squared error (RMSE) which is considered an excellent general purpose error metric for numerical predictions as given in (4), where n is the number of observations available for analysis, P_i are the predicted values of the variable and O_i are the observed values.

$$RMSE = \sqrt{\frac{1}{n}\sum_{i=1}^{n}(P_i - O_i)^2} \quad (4)$$

A low RMSE value meant that the predicted values were close to the real values and that the model could well predict the observations. Secondly, plotting of the residuals against the predictions of a model was done as a standard through which the model could be validated statistically because it was used as a measure of the distribution of errors. The interpretation of residual plots led to the acceptance or non-acceptance of the thin layer drying model. Generally, if the right model was used to determine the quality of fit, the residuals had a low band width and were close to the residual line. A model with residuals plot indicating a high band width was not accepted because it could not best describe the drying behaviour of black nightshade seeds.

2.6. Data Analysis

Microsoft 365 Excel software was used as a computational and graphical tool. Statistical analyses were carried out using R, version 4.1.3 [17]. Curve fitting to experimental data for thin layer drying models was performed using *mosaic* collection of packages in R language [18]. R Scripts and console outputs for coefficients, constants and RMSE in three modes of drying were generated in R [17].

3. Results and Discussion

Three sets of experiments were conducted by varying the drying modes—solar, solar-exhaust gas, and exhaust gas. In solar mode, Table 2 summarizes the data for the average hourly relative humidities, and temperatures—both inside and outside the dryer. Figure 5 is a plot of variations of the parameters in Table 2 with drying time of black nightshade seeds.

Table 2. *Average hourly data of the dryer parameters in solar mode.*

Drying Time (hours)	Outside RH (%)	Inside RH (%)	Outside Temperature (°C)	Inside Temperature (°C)
0	32.37	88.03	12.72	14.82
1	32.40	67.78	16.03	22.36
2	36.27	36.35	21.65	38.35
3	39.02	27.32	22.77	40.81
4	40.72	19.97	23.73	46.94
5	41.02	13.70	26.22	54.14
6	41.13	15.48	26.72	50.85
7	50.20	12.77	27.30	54.75
8	51.78	9.40	28.75	58.46
9	59.30	13.63	29.75	51.64
10	70.52	26.59	31.35	37.03
11	94.88	37.19	31.52	29.05

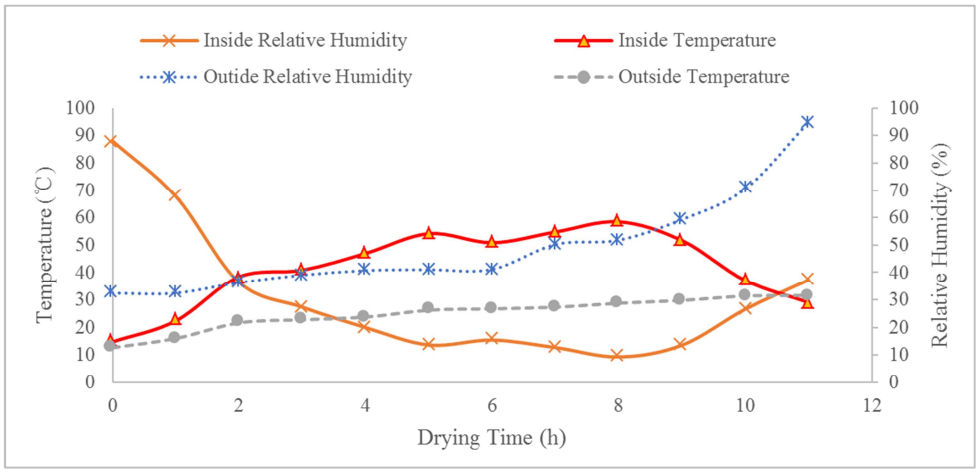

Figure 5. *Variations of dryer parameters with drying time in solar mode.*

From Figure 5 temperatures inside the dryer were higher than the corresponding outside temperatures throughout the drying period and this is because the cover material used in the dryer harnessed solar energy to keep the temperatures high. Previous authors [19, 5, 20-22] have reported that a combination of high temperature and low relative humidity in a dryer can increase the ability of drying air to perform well. In this mode, the temperature inside the dryer was observed to be high when the relative humidity inside the dryer was low. This phenomenon occurred as illustrated in Figure 5 for the drying time between 2-11 hours. In solar-exhaust gas mode, Table 3 summarizes the data for the average hourly relative humidities, and temperatures—both inside and outside the dryer. Figure 6 is a plot of variations of the parameters in Table 3 with drying time of black nightshade seeds.

Table 3. *Average hourly data of the dryer parameters in solar-exhaust gas mode.*

Drying Time (hours)	Outside RH (%)	Inside RH (%)	Outside Temperature (°C)	Inside Temperature (°C)
0	68.15	39.27	20.75	34.49
1	53.93	27.19	24.80	41.79
2	40.13	14.84	28.80	50.05
3	40.13	14.84	28.80	50.05
4	13.35	11.78	47.65	51.93
5	9.88	12.27	53.00	58.61
6	9.55	9.55	51.05	61.97
7	9.15	7.68	51.65	61.49
8	8.75	7.10	52.48	59.64
9	11.20	7.31	47.95	58.75
10	10.95	8.29	48.55	56.34

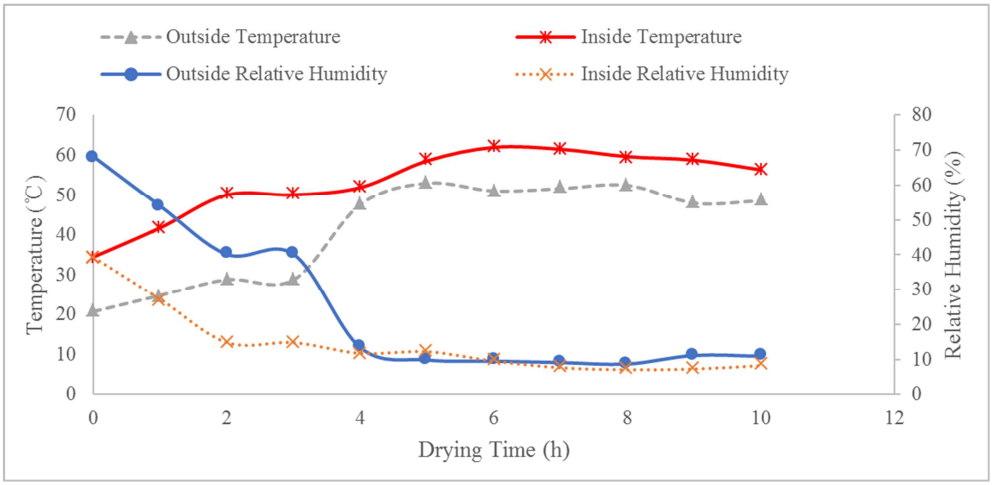

Figure 6. *Variations of dryer parameters with drying time in solar-exhaust gas mode.*

Table 4. *Average hourly data of the dryer parameters in exhaust gas mode.*

Drying Time (hours)	Outside RH (%)	Inside RH (%)	Outside Temperature (°C)	Inside Temperature (°C)
0	54.70	51.88	22.05	25.75
1	58.05	59.80	21.35	27.50
2	61.40	67.28	20.85	28.26
3	63.85	76.37	20.50	28.62
4	67.70	83.98	19.85	29.26
5	69.55	74.25	19.60	28.62
6	69.55	74.25	19.60	28.62
7	55.50	59.66	22.20	30.77
8	57.55	72.85	21.85	30.65
9	58.60	71.77	21.55	30.50
10	60.30	70.31	21.30	30.60
11	61.60	67.25	20.90	28.53
12	63.50	68.10	20.50	28.28
13	66.20	76.82	20.10	28.43
14	66.20	76.98	19.90	28.34

From Figure 6 temperatures inside the dryer were higher than the corresponding outside temperatures throughout the drying period and this is because the cover material used in the dryer harnessed solar energy to raise the temperature

while at the same time heat energy recovered from exhaust gas of a diesel engine kept the temperatures high. Inside relative humidity was low as compared to the outside relative humidity for the first four hours of dying. It is within these hours that fast rate of moisture loss from the product were observed (Figure 9, Figure 11). The relative humidity trend for the remaining hours of drying showed relative equality but were still low for the drying air to be effective in drying—a combination of high temperature and low relative humidity in a dryer can increase the ability of drying air to carry away moisture. In summary, for this mode, the temperature inside the dryer was observed to be high when the relative humidity inside the dryer was low as illustrated in Figure 6 for the entire drying period. In exhaust gas mode, Table 4 summarizes the data for the average hourly relative humidities, and temperatures—both inside and outside the dryer. Figure 7 is a plot of variations of the parameters in Table 4 with drying time of black nightshade seeds.

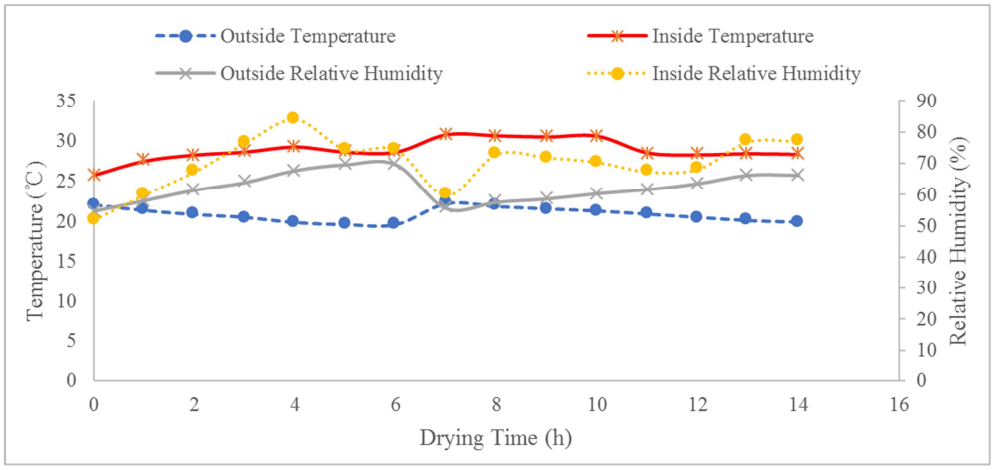

Figure 7. *Variations of dryer parameters with drying time in exhaust mode.*

From Figure 7 temperatures inside the dryer were higher than the corresponding outside temperatures throughout the drying period and this is because heat energy recovered from exhaust gas of a diesel engine kept the temperatures high. However, relative humidity inside the dryer were higher than those outside because water vapour from the open cooling system of a diesel engine kept the dryer moist. Increase in relative humidity inside the dryer was not suitable for quick drying, therefore, the drying period for the mode was 14 hours, a longer period as compared to solar-exhaust gas drying mode where the product was dried in 10 hours (Figure 11). With reference to the outside and inside temperatures of this mode of drying, the average hourly rise in temperature inside the dryer was 8.04°C with a minimum rise of 3.7°C and a maximum of 9.41°C when exhaust gas was utilized to provide heat energy. The results of mass change of black nightshade seeds with time are presented in Tables 5, 6 and 7 for the corresponding drying modes. Figures 8, 9 and 10 illustrate the results of variation of moisture content and drying rate—with drying time—of black nightshade seeds during solar, solar-exhaust gas, and exhaust gas modes of drying respectively. Fast rates of moisture loss were observed within the first four hours and thereafter the rates slowed down. Similar trends of drying rates have been observed by Ronoh *et al.* [5] who reported that the drying process can be divided into three periods: a short primary increasing, a fairly constant and a falling drying rate. From Figures 8 to 10 it can be observed that the falling rate period clearly dominated the drying process of black nightshade seeds. Such a dominant falling rate period is attributed to diffusion mechanisms that control drying of agricultural produce. Continuous decrease in drying rate with decreasing moisture content—increasing drying time—was observed in all the drying modes. Similar observations have been reported by authors who have previously dried agricultural produce [19, 5, 20, 23, 21, 6].

Table 5. *Change in mass of black nightshade seeds during solar mode of drying.*

Time (h)	Mass (g)	Moisture Content (% db)	Drying Rate (g/g/h)	Moisture Ratio
0	50.00	89.34	0	1
1	29.20	71.2329	5.1106	0.7973
2	18.67	56.4006	2.5872	0.6313
3	12.97	43.9476	1.4005	0.4919
4	9.83	31.9430	0.7715	0.3575
5	7.92	24.1162	0.4693	0.2699
6	6.62	19.6375	0.3194	0.2198
7	5.78	14.5329	0.2064	0.1627
8	5.17	11.7988	0.1499	0.1321
9	4.71	9.7665	0.1130	0.1093
10	4.36	8.0275	0.0860	0.0899
11	4.07	7.1253	0.0713	0.0798

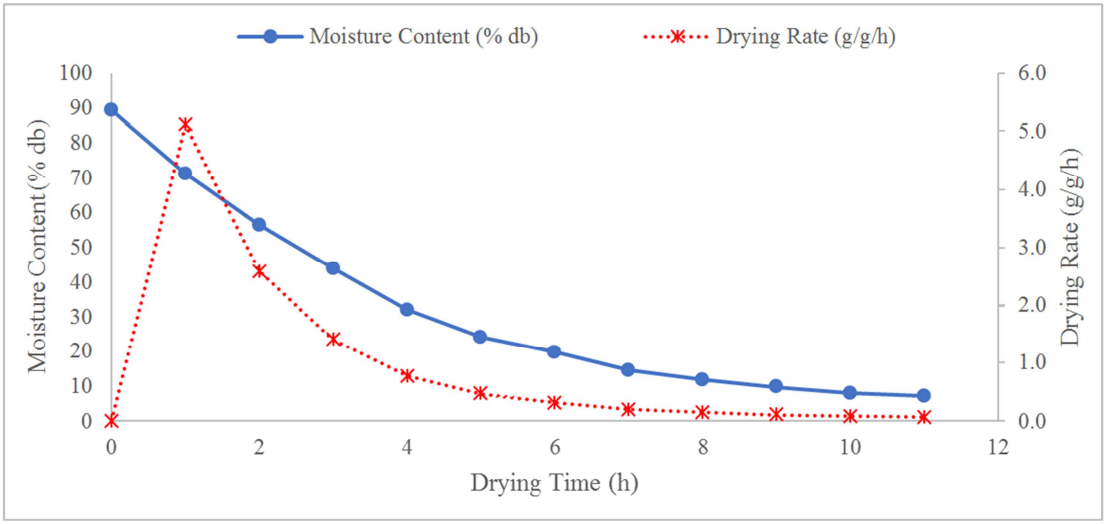

Figure 8. *Moisture content and drying rate variations with drying time in solar mode.*

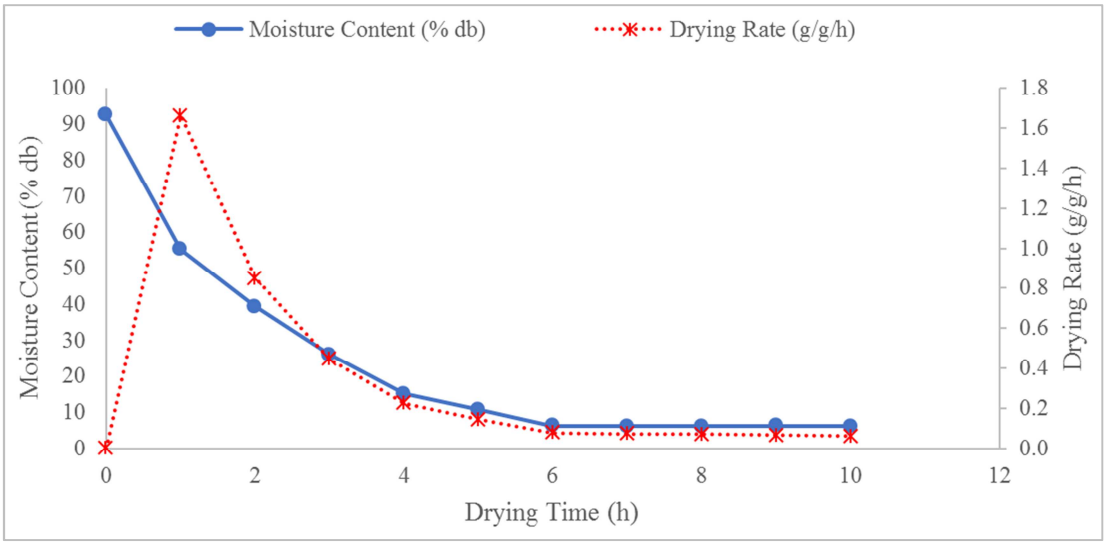

Figure 9. *Moisture content and drying rate variations with drying time in solar-exhaust gas mode.*

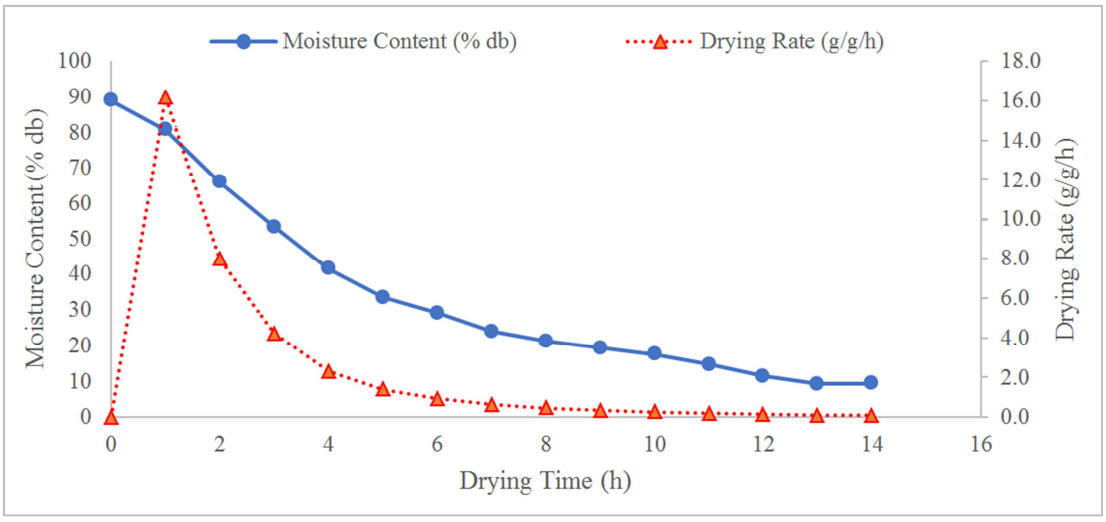

Figure 10. *Moisture content and drying rate variations with drying time in exhaust gas mode.*

Table 6. *Change in mass of black nightshade seeds during solar-exhaust gas mode of drying.*

Time (h)	Mass (g)	Moisture Content (% db)	Drying Rate (g/g/h)	Moisture Ratio
0	50.00	92.57	0	1
1	32.21	55.2313	1.6626	0.5966
2	23.12	39.3166	0.8495	0.4247
3	18.36	25.9259	0.4449	0.2801
4	15.95	15.1097	0.2252	0.1632
5	14.41	10.6870	0.1439	0.1154
6	13.57	6.1901	0.0785	0.0669
7	12.79	6.0985	0.0729	0.0659
8	12.05	6.1411	0.0692	0.0663
9	11.35	6.1674	0.0654	0.0666
10	10.70	6.0748	0.0607	0.0656

Table 7. *Change in mass of black nightshade seeds during exhaust gas mode of drying.*

Time (h)	Mass (g)	Moisture Content (% db)	Drying Rate (g/g/h)	Moisture Ratio
0	50.00	88.84	0	1
1	27.67	80.7011	16.1812	0.9084
2	16.67	65.9868	7.9710	0.7428
3	10.87	53.3579	4.2029	0.6006
4	7.68	41.5365	2.3116	0.4675
5	5.75	33.5652	1.3986	0.3778
6	4.45	29.2135	0.9420	0.3288
7	3.59	23.9554	0.6232	0.2696
8	2.96	21.2838	0.4565	0.2396
9	2.48	19.3548	0.3478	0.2179
10	2.11	17.5355	0.2681	0.1974
11	1.84	14.6739	0.1957	0.1652
12	1.65	11.5152	0.1377	0.1296
13	1.51	9.2715	0.1014	0.1044
14	1.38	9.4203	0.0942	0.1060

Figure 11 illustrates the comparison of drying time for the three modes of drying. Moisture ratio variation with time show that the solar-exhaust gas mode of drying took the shortest time at 10 hours. This was followed by solar mode of drying at 11 hours and finally exhaust gas mode of drying took the longest at 14 hours. These drying times can be explained by the relative humidity and temperature variations, inside and outside the dryer, with time as presented in Tables 2 to 4 and illustrated in Figures 5 to 7.

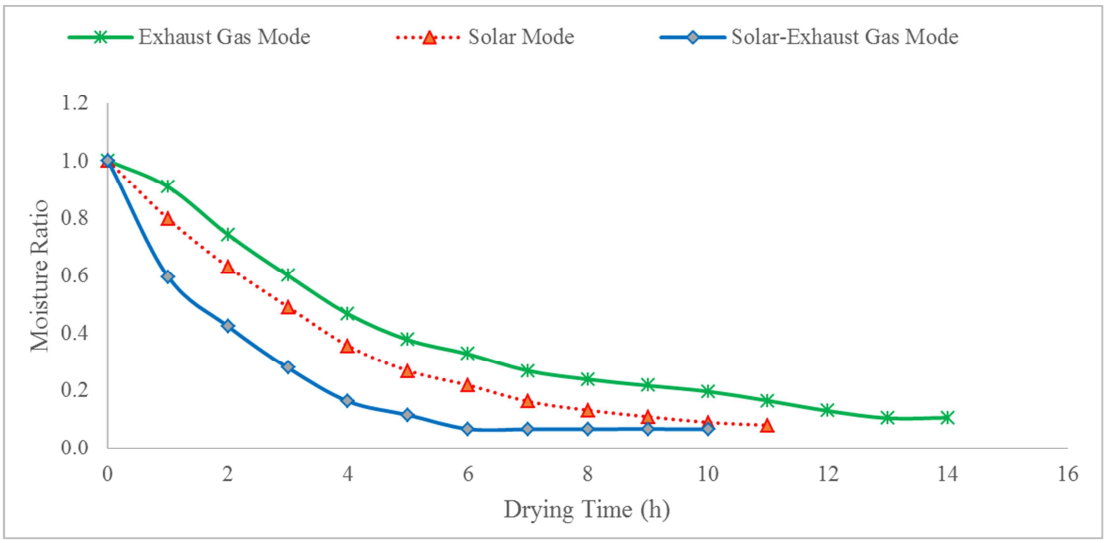

Figure 11. *Drying time comparison for solar, solar-exhaust gas, and exhaust gas modes of drying.*

Tables 8, 9 and 10 show the coefficients, constants and RMSE values for thin layer drying models selected for this work in solar, solar-exhaust gas, and exhaust gas modes respectively. From Table 8, it can be observed that Page model with the lowest RMSE value was the most appropriate in describing drying kinetics of black nightshade seeds when the dryer was operated on solar mode. Similar results for suitability of Page model in characterizing agricultural

produce have been reported during thin layer drying studies of various food materials, including jackfruit slices [5], tomato slices [24], pineapple [23], banana [25], chili [26], rapeseed [27], amaranth [28], sultana grapes [29]. From Table 9, in solar-exhaust gas mode of drying, Logarithmic model had the lowest value of RMSE compared to the other three thin layer drying models. Accordingly, Logarithmic model was selected to best characterize the thin layer drying of black nightshade seeds in the mode. Similarly, from Table 10, in exhaust gas mode Logarithmic model with the lowest RMSE value was the most appropriate in describing the drying kinetics of the seeds.

Table 8. *Thin layer drying models' coefficients, constants and RMSE for solar mode.*

Model	Coefficients and Constants	RMSE
Newton	k = 0.247807	0.01328758
Page	k = 0.2318547, n = 1.0435172	0.01147206
Logarithmic	k = 0.253920354, a = 1.010375048, c = 0.004154843	0.01234601
Henderson and Pabis	k = 0.2512012, a = 1.0133079	0.01239765

Table 9. *Thin layer drying models' coefficients, constants and RMSE for solar-exhaust gas mode.*

Model	Coefficients and Constants	RMSE
Newton	k = 0.4354244	0.02927717
Page	k = 0.5057220, n = 0.8586389	0.02208625
Logarithmic	k = 0.4948986, a = 0.9501944, c = 0.0443512	0.0172098
Henderson and Pabis	k = 0.4255844, a = 0.9777158	0.02835186

Table 10. *Thin layer drying models' coefficients, constants and RMSE for exhaust gas mode.*

Model	Coefficients and Constants	RMSE
Newton	k = 0.1747693	0.02734447
Page	k = 0.1653073, n = 1.0305292	0.02688727
Logarithmic	k = 0.2011363, a = 1.0001196, c = 0.0423407	0.02315325
Henderson and Pabis	k = 0.1801766, a = 1.0284582	0.02543765

Tables 11, 12 and 13 show the experimental and predicted moisture ratios by thin layer drying models selected for this work in solar, solar-exhaust gas, and exhaust gas modes respectively.

Table 11. *Experimental and predicted moisture ratios data in solar mode of drying.*

Time (h)	Experimental	Newton	Page	Logarithmic	Henderson and Pabis
0	1	1	1	1.0145	1.0133
1	0.7973	0.7805	0.7931	0.7880	0.7882
2	0.6313	0.6092	0.6201	0.6122	0.6131
3	0.4919	0.4755	0.4821	0.4758	0.4769
4	0.3575	0.3711	0.3734	0.3701	0.3710
5	0.2699	0.2897	0.2884	0.2880	0.2886
6	0.2198	0.2261	0.2223	0.2244	0.2245
7	0.1627	0.1765	0.1709	0.1750	0.1746
8	0.1321	0.1377	0.1313	0.1367	0.1358
9	0.1093	0.1075	0.1007	0.1070	0.1057
10	0.0899	0.0839	0.0771	0.0839	0.0822
11	0.0798	0.0655	0.0590	0.0660	0.0639

Table 12. *Experimental and predicted moisture ratios data for solar-exhaust mode of drying.*

Time (h)	Experimental	Newton	Page	Logarithmic	Henderson and Pabis
0	1	1	1	0.9945	0.9777
1	0.5966	0.6470	0.6031	0.6236	0.6388
2	0.4247	0.4186	0.3997	0.3975	0.4174
3	0.2801	0.2708	0.2728	0.2596	0.2727
4	0.1632	0.1752	0.1896	0.1756	0.1782
5	0.1154	0.1134	0.1334	0.1244	0.1164
6	0.0669	0.0733	0.0949	0.0931	0.0761
7	0.0659	0.0475	0.0680	0.0741	0.0497
8	0.0663	0.0307	0.0490	0.0625	0.0325
9	0.0666	0.0199	0.0356	0.0554	0.0212
10	0.0656	0.0129	0.0259	0.0511	0.0139

Table 13. *Experimental and predicted moisture ratios data for exhaust mode of drying.*

Time (h)	Experimental	Newton	Page	Logarithmic	Henderson and Pabis
0	1	1	1	1.0425	1.0285
1	0.9084	0.8397	0.8476	0.8602	0.8589
2	0.7428	0.7050	0.7134	0.7112	0.7173
3	0.6006	0.5920	0.5988	0.5894	0.5990
4	0.4675	0.4970	0.5017	0.4897	0.5003
5	0.3778	0.4173	0.4197	0.4082	0.4178
6	0.3288	0.3504	0.3508	0.3415	0.3489
7	0.2696	0.2942	0.2929	0.2870	0.2914
8	0.2396	0.2471	0.2444	0.2424	0.2433
9	0.2179	0.2074	0.2037	0.2060	0.2032
10	0.1974	0.1742	0.1697	0.1762	0.1697
11	0.1652	0.1462	0.1414	0.1518	0.1417
12	0.1296	0.1228	0.1177	0.1318	0.1184
13	0.1044	0.1031	0.0979	0.1155	0.0988
14	0.1060	0.0866	0.0814	0.1022	0.0825

Figure 12 illustrates Newton model fitting to experimental data in solar mode of drying while Figure 13 shows the residual plots as a variation with the model's predictions. Residual plots were performed to show the model's appropriateness in describing the drying kinetics of black nightshade seeds in solar mode of drying. From Figure 13, considering a band width of ±0.015, Newton model had 8 out of the possible 12 data points for the predicted moisture ratio close to the residual line. Out of 12 predicted data points, 1 fell directly on the residual line. However, for this model, out of the four thin layer drying models considered in this mode of drying, it was fourth in performance.

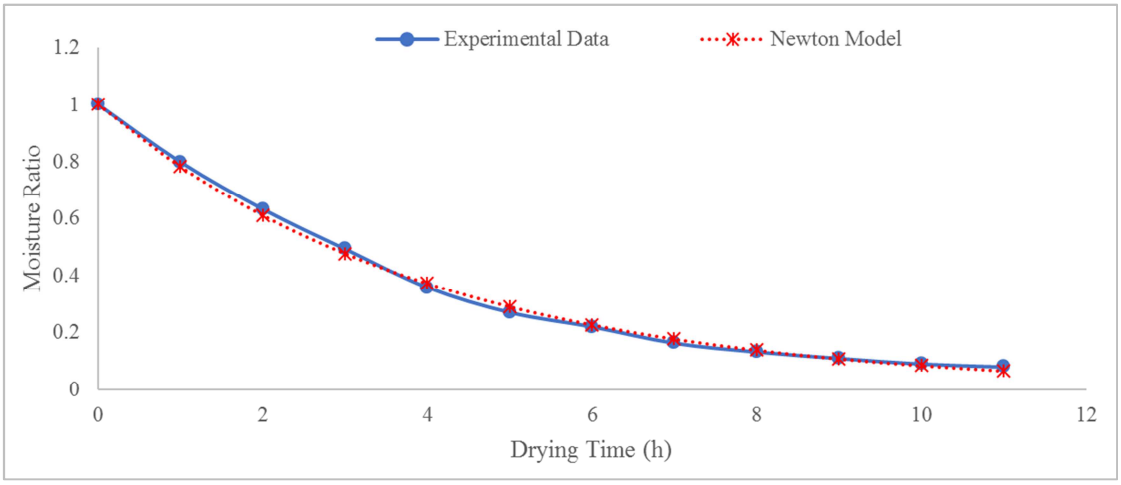

Figure 12. *Newton model fitting to experimental data in solar mode of drying.*

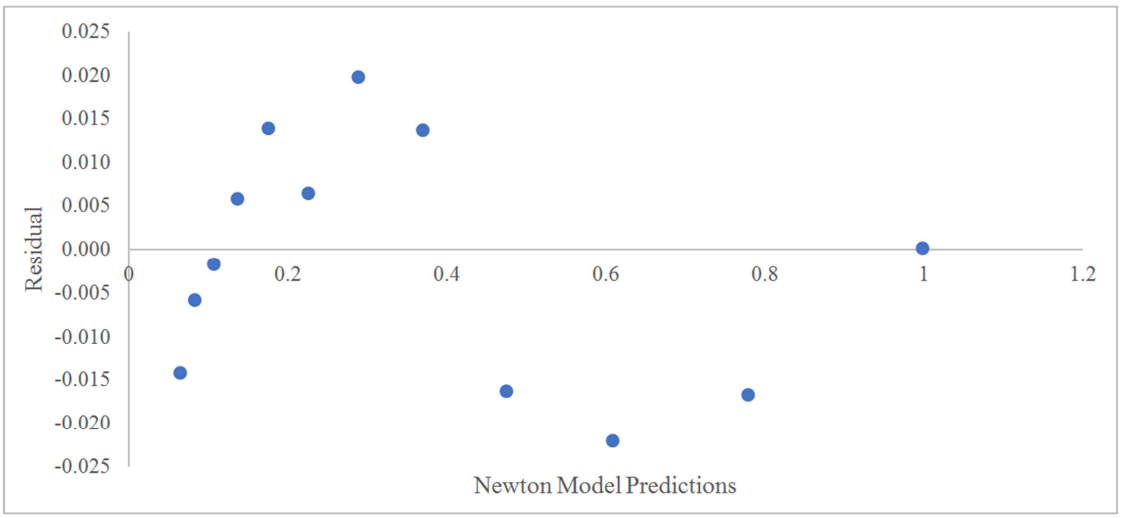

Figure 13. *Newton model predictions and residual plots in solar mode of drying.*

Figure 14 illustrates the Page model fitting to experimental data in solar mode of drying while Figure 15 shows the residual plots as a variation with the model's predictions. Residual plots were performed to show the model's appropriateness in describing drying kinetics of black nightshade seeds in solar mode of drying. Unlike other thin layer drying models considered in this mode, Page model, from Figure 15, had 10 out of the possible 12 predicted data points for moisture ratio close to the residual line within a band width of ± 0.015. Out of the 12 predicted data points, 2 fell directly on the residual line, therefore, this model was the most appropriate in describing thin layer drying of black nightshade seeds when drying was performed in solar mode.

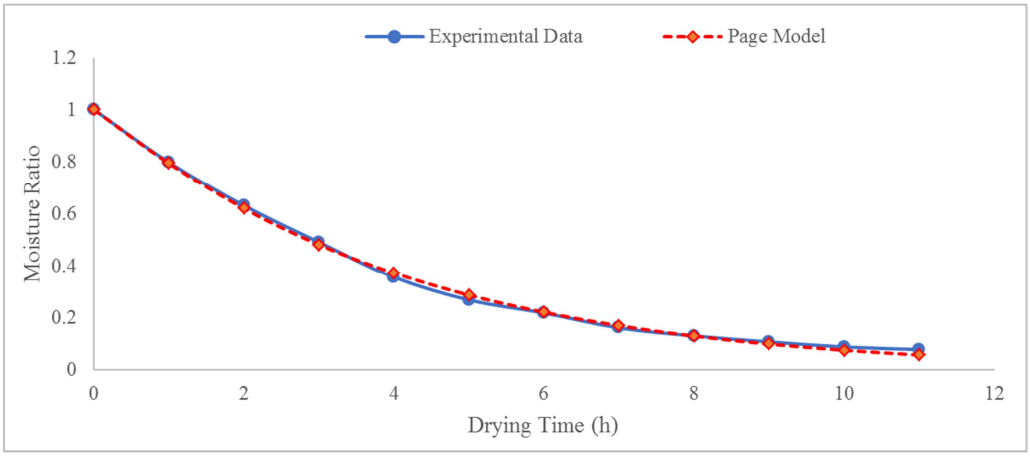

Figure 14. *Page model fitting to experimental data in solar mode of drying.*

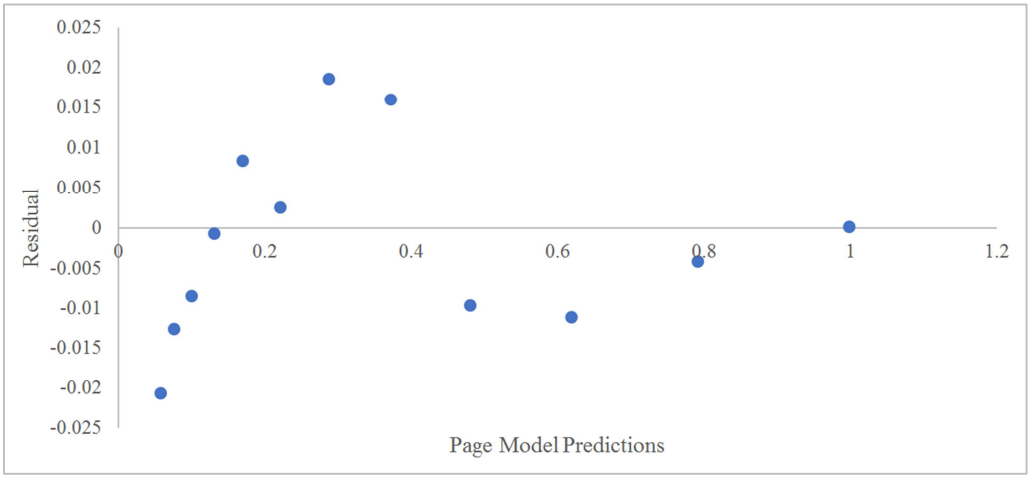

Figure 15. *Page model predictions and residual plots in solar mode of drying.*

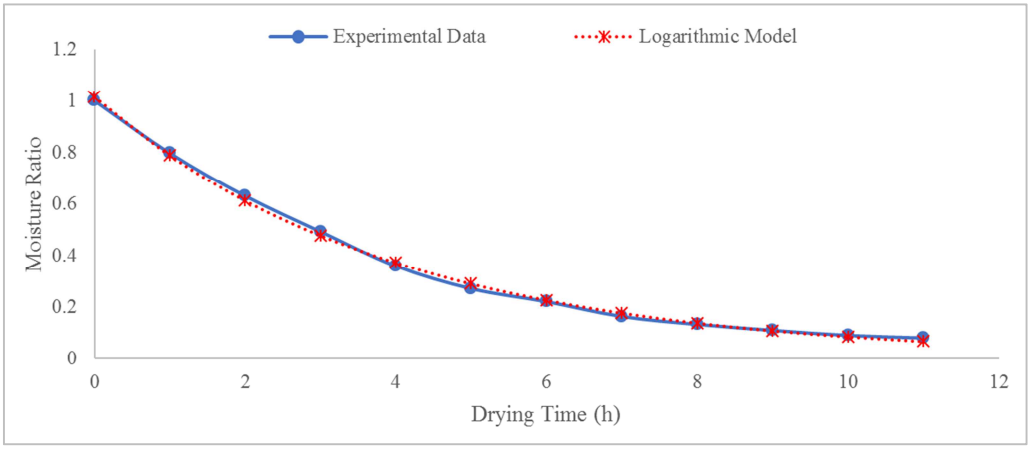

Figure 16. *Logarithmic model fitting to experimental data in solar mode of drying.*

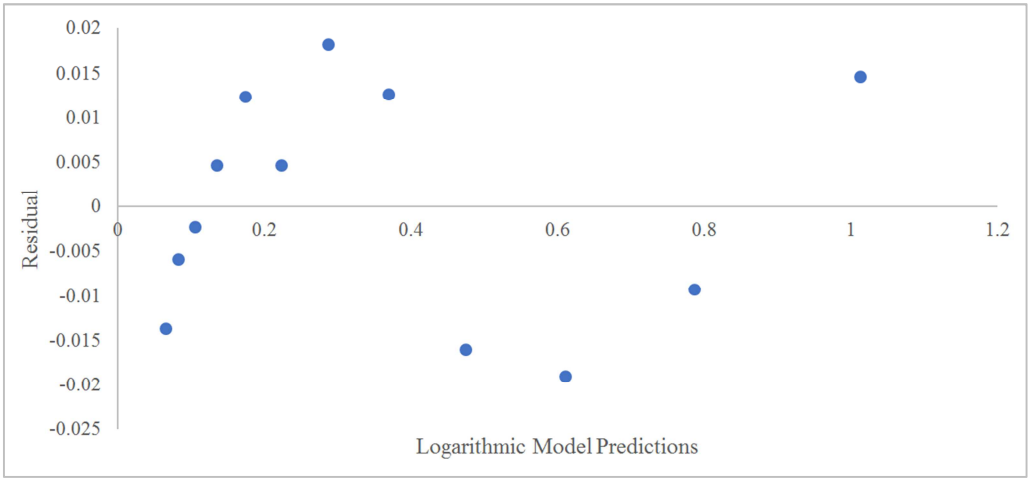

Figure 17. *Logarithmic model predictions and residual plots in solar mode of drying.*

Figure 16 illustrates Logarithmic model fitting to experimental data in solar mode of drying while Figure 17 shows the residual plots as a variation with the model's predictions. Residual plots were performed to show the model's appropriateness in describing the drying kinetics of black nightshade seeds in solar mode of drying. From Figure 17, considering a band width of ±0.015, Logarithmic model had 9 out of the possible 12 data points for the predicted moisture ratio close to the residual line. Out of 12 predicted data points, none fell directly on the residual line. However, for this model, out of the four thin layer drying models considered in this mode of drying, it was second in performance.

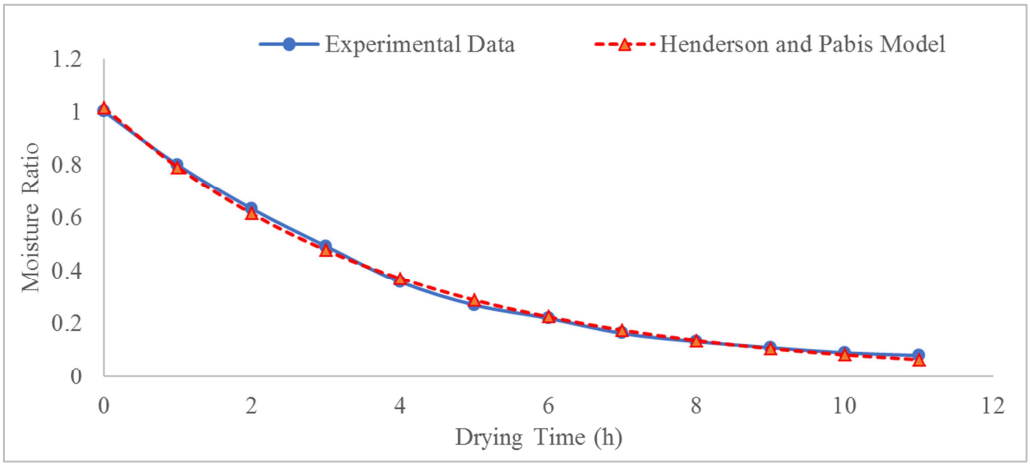

Figure 18. *Henderson and Pabis model fitting to experimental data in solar mode of drying.*

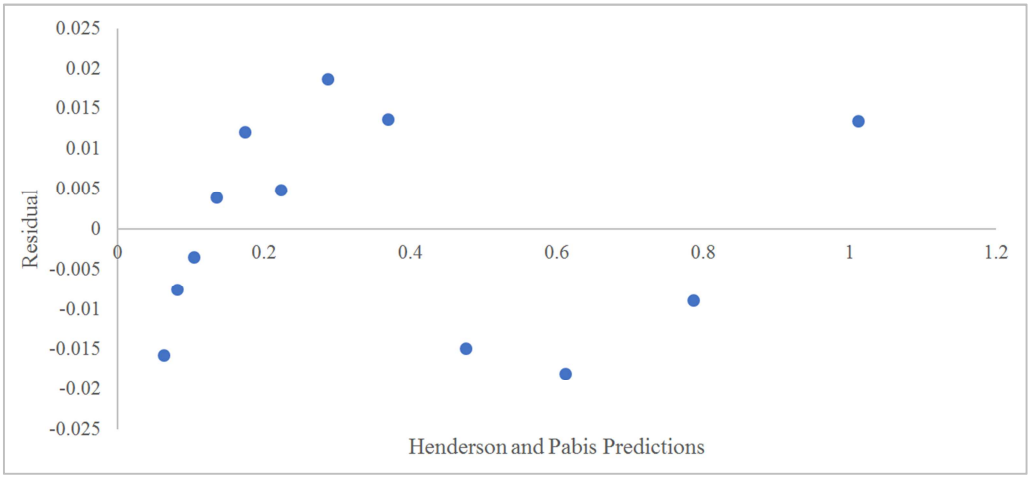

Figure 19. *Henderson and Pabis model predictions and residual plots in solar mode of drying.*

Figure 18 illustrates Henderson and Pabis model fitting to experimental data in solar mode of drying while Figure 19 shows the residual plots as a variation with the model's predictions. Residual plots were performed to show the model's appropriateness in describing the drying kinetics of black nightshade seeds in solar mode of drying. From Figure 19 the performance of Henderson and Pabis was almost similar to Logarithmic model when the product was dried in solar mode. Considering a band width of ± 0.015, Henderson and Pabis model had 9 out of the possible 12 data points for the predicted moisture ratio close to the residual line. Out of 12 predicted data points, none fell directly on the residual line. However, for this model, out of the four thin layer drying models considered in this mode of drying, it was third in performance.

Figure 20 illustrates Newton model fitting to experimental data in solar-exhaust gas mode of drying while Figure 21 shows the residual plots as a variation with the model's predictions. Residual plots were performed to show the model's appropriateness in describing the drying kinetics of black nightshade seeds in solar-exhaust gas mode of drying. From Figure 21, considering a band width of ± 0.015, Newton model had 6 out of the possible 11 data points for the predicted moisture ratio close to the residual line. Out of 11 predicted data points, 1 fell directly on the residual line. However, for this model, out of the four thin layer drying models considered in this mode of drying, it was fourth in performance because 4 out of 11 of the predicted values were outside the band width of ± 0.03.

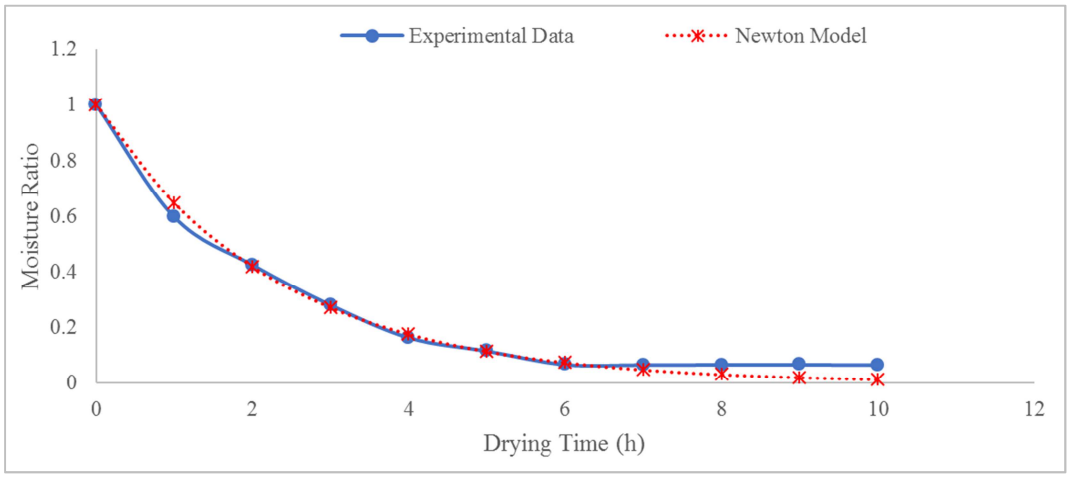

Figure 20. *Newton model fitting to experimental data in solar-exhaust gas mode of drying.*

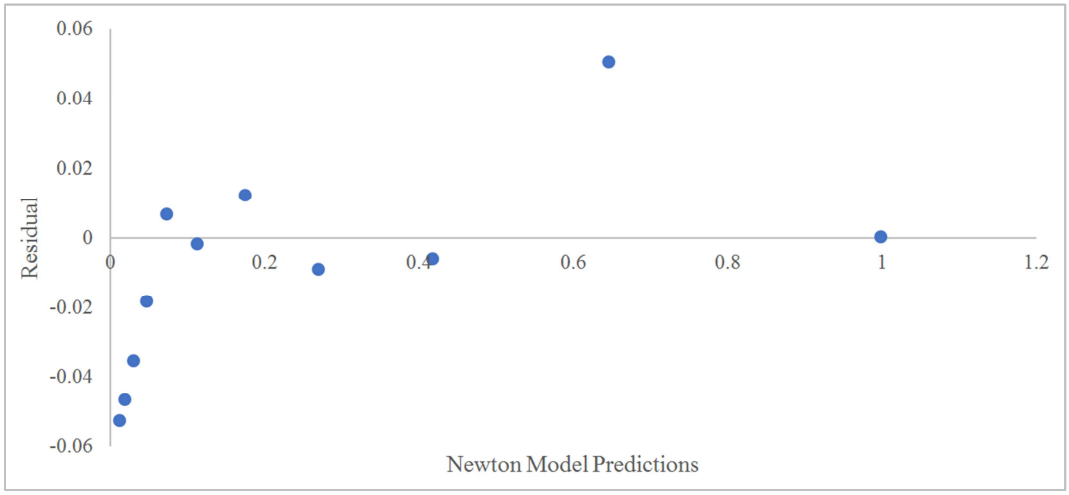

Figure 21. *Newton model predictions and residual plots in solar-exhaust gas mode of drying.*

Figure 22 illustrates Page model fitting to experimental data in solar-exhaust gas mode of drying while Figure 23 shows the residual plots as a variation with the model's predictions. Residual plots were performed to show the model's appropriateness in describing drying kinetics of black nightshade seeds in solar-exhaust gas mode of drying. From Figure 23, considering a band width of ± 0.015, Page model had 4 out of the possible 11 data points for the predicted moisture ratio close to the residual line. Out of 11 predicted data points, 1 fell directly on the residual line. However, for this model, out of the four thin layer drying models considered in this mode of drying, it was second in performance because 2 out of 11 of the predicted values were outside the band width of ± 0.03.

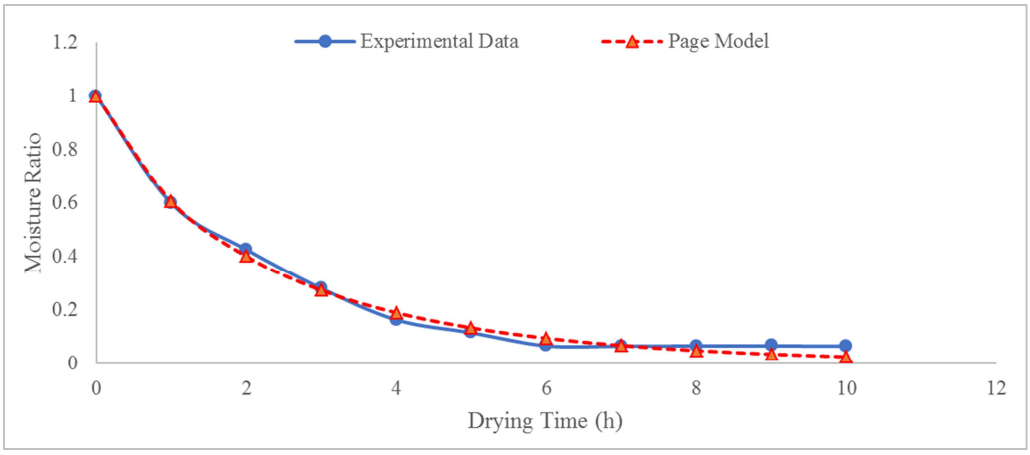

Figure 22. *Page model fitting to experimental data in solar-exhaust gas mode of drying.*

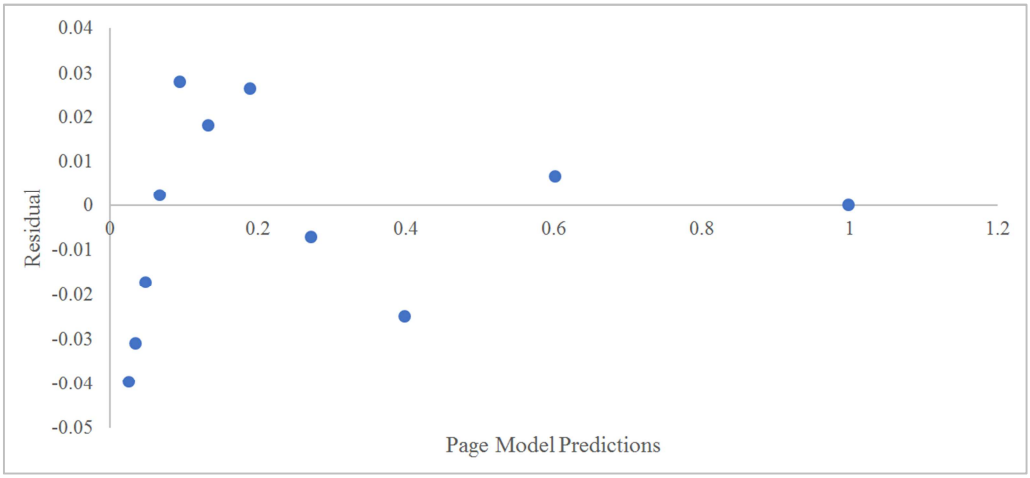

Figure 23. *Page model predictions and residual plots in solar-exhaust gas mode of drying.*

Figure 24 illustrates Logarithmic model fitting to experimental data in solar-exhaust gas mode of drying while Figure 25 shows the residual plots as a variation with the model's predictions. Residual plots were performed to show the model's appropriateness in describing the drying kinetics of black nightshade seeds in solar-exhaust gas mode of drying. Unlike other thin layer drying models considered in this mode, Logarithmic model, from Figure 25, had 6 out of the possible 11 predicted data points for moisture ratio close to the residual line within a band width of ± 0.015. Out of the 11 predicted data points, none fell directly on the residual line, however, this model was the most appropriate in describing thin layer drying of black nightshade seeds when drying was performed in solar-exhaust mode because none out of 11 of the predicted values were outside the band width of ± 0.03.

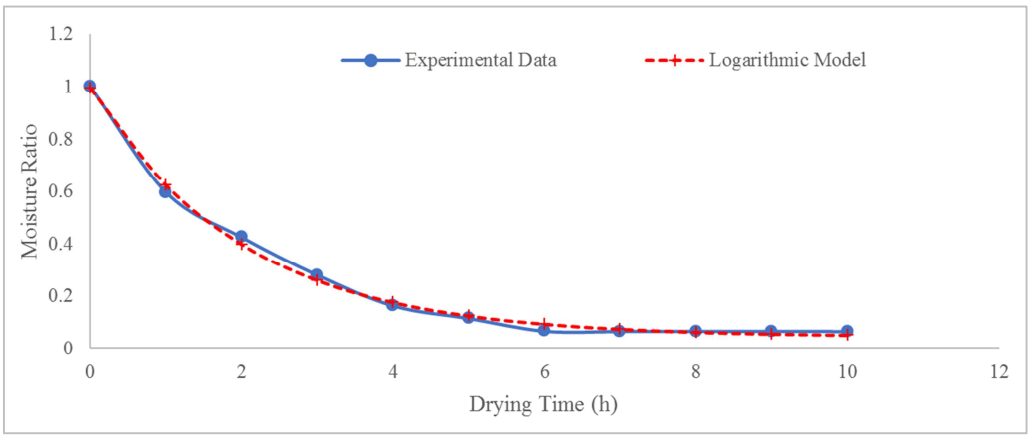

Figure 24. *Logarithmic model fitting to experimental data in solar-exhaust gas mode of drying.*

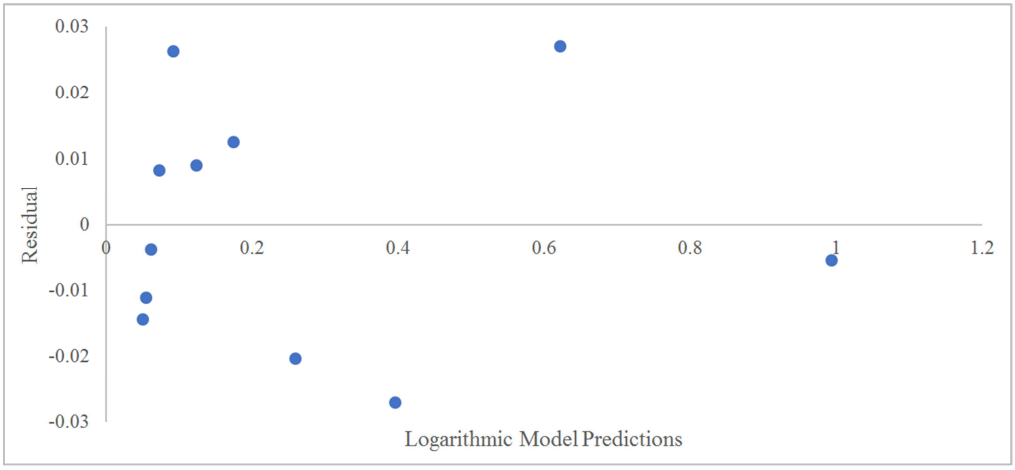

Figure 25. *Logarithmic model predictions and residual plots in solar-exhaust gas mode of drying.*

Figure 26 illustrates Henderson and Pabis model fitting to experimental data in solar-exhaust gas mode of drying while Figure 27 shows the residual plots as a variation with the model's predictions. Residual plots were performed to show the model's appropriateness in describing the drying kinetics of black nightshade seeds in solar-exhaust gas mode of drying. From Figure 27, considering a band width of ± 0.015, Henderson and Pabis model had 5 out of the possible 11 data points for the predicted moisture ratio close to the residual line. Out of 11 predicted data points, 1 fell directly on the residual line. However, for this model, out of the four thin layer drying models considered in this mode of drying, it was third in performance because 4 out of 11 of the predicted values were outside the band width of ± 0.03.

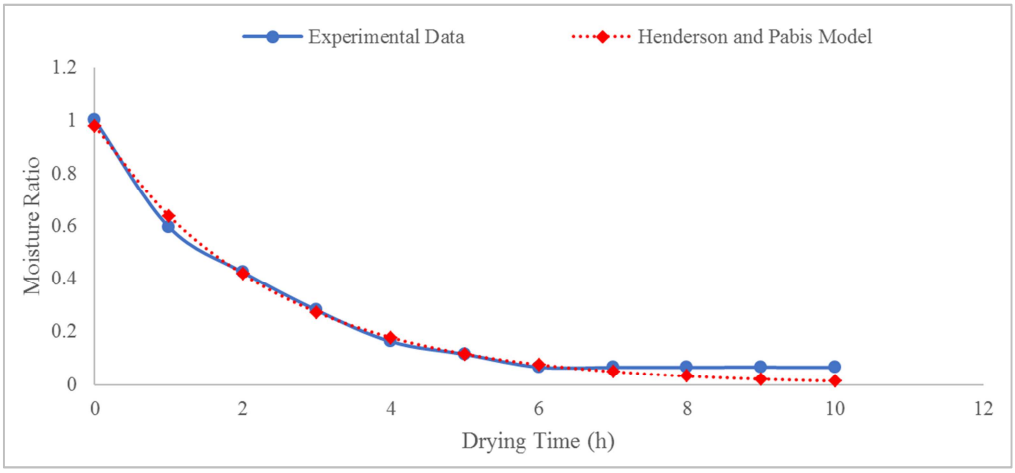

Figure 26. *Henderson and Pabis model fitting to experimental data in solar-exhaust gas mode of drying.*

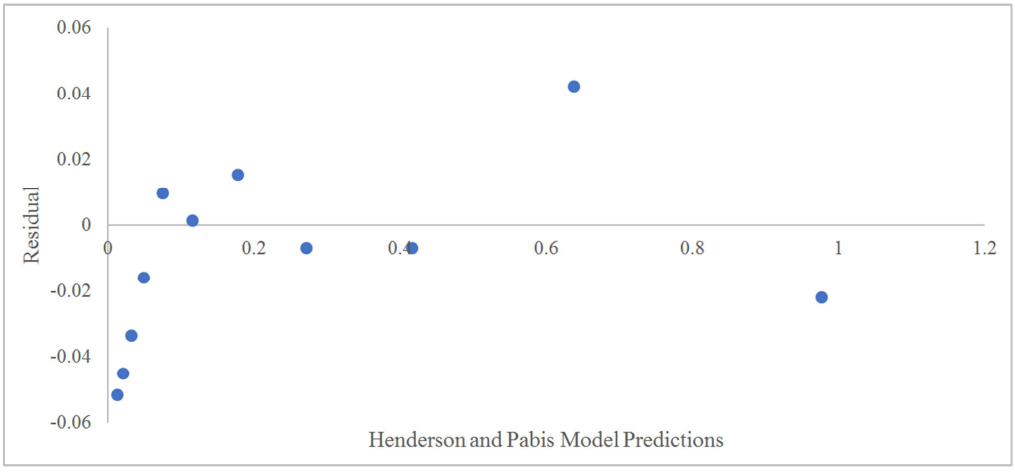

Figure 27. *Henderson and Pabis model predictions and residual plots in solar-exhaust gas mode of drying.*

Figure 28 illustrates the Newton model fitting to experimental data in exhaust gas mode of drying while Figure 29 shows the residual plots as a variation with the model's predictions. Residual plots were performed to show the model's appropriateness in describing the drying kinetics of black nightshade seeds in exhaust gas mode of drying. From Figure 29, considering a band width of ± 0.015, Newton model had 6 out of the possible 15 data points for the predicted moisture ratio close to the residual line. Out of 15 predicted data points, 2 fell directly on the residual line. However, for this model, out of the four thin layer drying models considered in this mode of drying, it was fourth in performance because 3 out of 15 of the predicted values were outside the band width of ± 0.03.

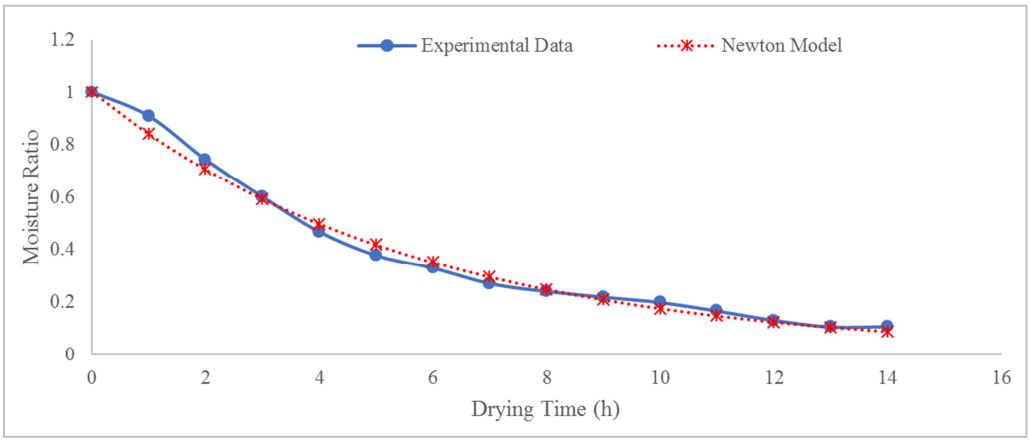

Figure 28. *Newton model fitting to experimental data in exhaust gas mode of drying.*

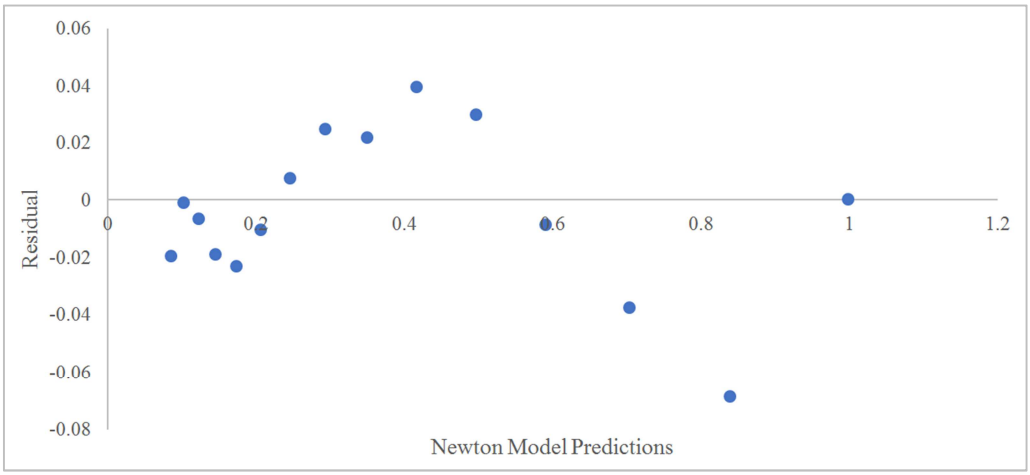

Figure 29. *Newton model predictions and residual plots in exhaust gas mode of drying.*

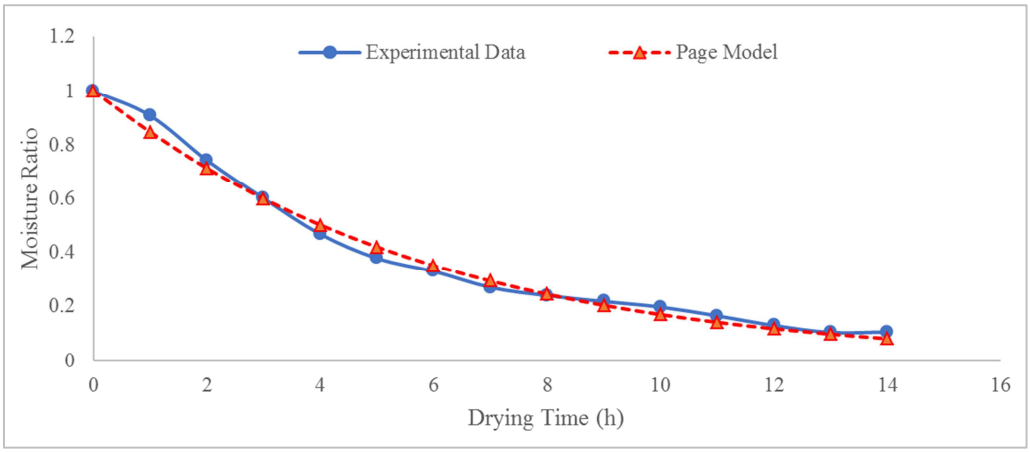

Figure 30. *Page model fitting to experimental data in exhaust gas mode of drying.*

Figure 30 illustrates the Page model fitting to experimental data in exhaust gas mode of drying while Figure 31 shows the residual plots as a variation with the model's predictions. Residual plots were performed to show the model's appropriateness in describing the drying kinetics of black nightshade seeds in exhaust gas mode of drying. This model performed almost similar to Newton model based on the residual plots. From Figure 31, considering a band width of ±0.015, Page model had 6 out of the possible 15 data points for the predicted moisture ratio close to the residual line. Out of 15 predicted data points, 2 fell directly on the residual line. However, for this model, out of the four thin layer drying models considered in this mode of drying, it was third in performance because 3 out of 15 of the predicted values were outside the band width of ±0.03.

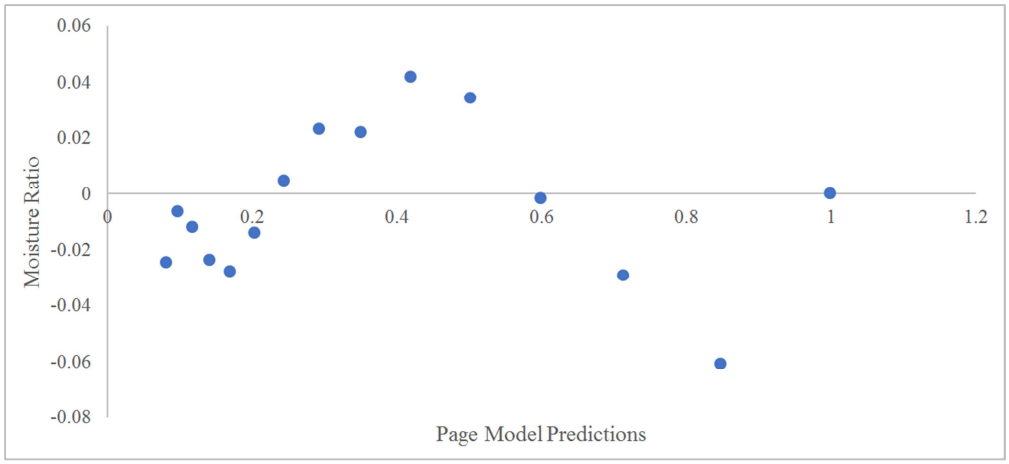

Figure 31. *Page model predictions and residual plots in exhaust gas mode of drying.*

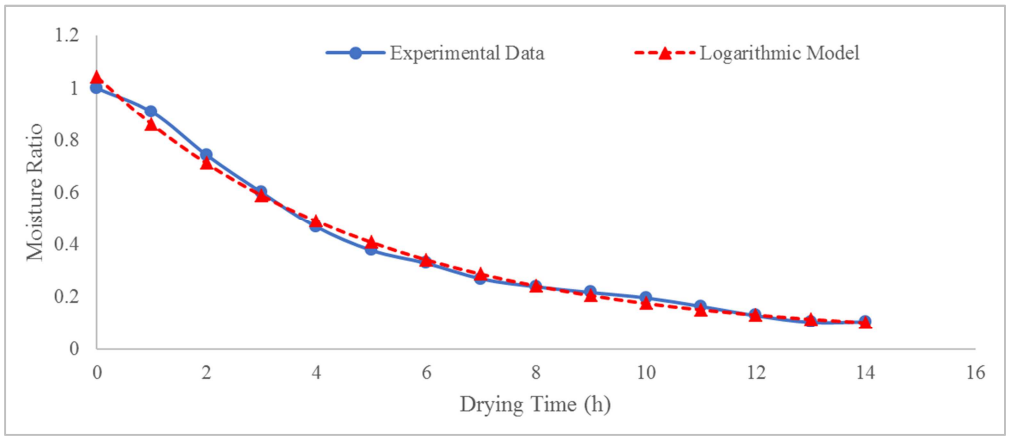

Figure 32. *Logarithmic model fitting to experimental data in exhaust gas mode of drying.*

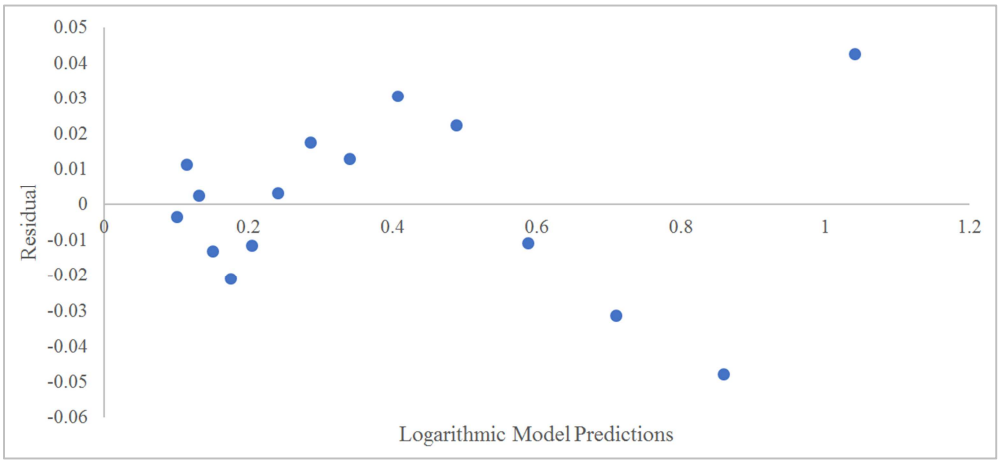

Figure 33. *Logarithmic model predictions and residual plots in exhaust gas mode of drying.*

Figure 32 illustrates Logarithmic model fitting to experimental data in exhaust gas mode of drying while Figure 33 shows the residual plots as a variation with the model's predictions. Residual plots were performed to show the model's appropriateness in describing the drying kinetics of black nightshade seeds in exhaust gas mode of drying. Unlike other thin layer drying models considered in this mode, Logarithmic model, from Figure 33, had 8 out of the possible 15 predicted data points for moisture ratio close to the residual line within a band width of ± 0.015. Out of the 15 predicted data points, none fell directly on the residual line, however, this model was the most appropriate in describing thin layer drying of black nightshade seeds when drying was performed in exhaust mode because 2 out of 15 of the predicted values were outside the band width of ± 0.03.

Figure 34 illustrates Henderson and Pabis model fitting to experimental data in exhaust gas mode of drying while Figure 35 shows the residual plots as a variation with the model's predictions. Residual plots were performed to show the model's appropriateness in describing the drying kinetics of black nightshade seeds in exhaust gas mode of drying. From Figure 35, considering a band width of ± 0.015, Page model had 5 out of the possible 15 data points for the predicted moisture ratio close to the residual line. Out of 15 predicted data points, none fell directly on the residual line. However, for this model, out of the four thin layer drying models considered in this mode of drying, it was second in performance because 3 out of 15 of the predicted values were outside the band width of ± 0.03.

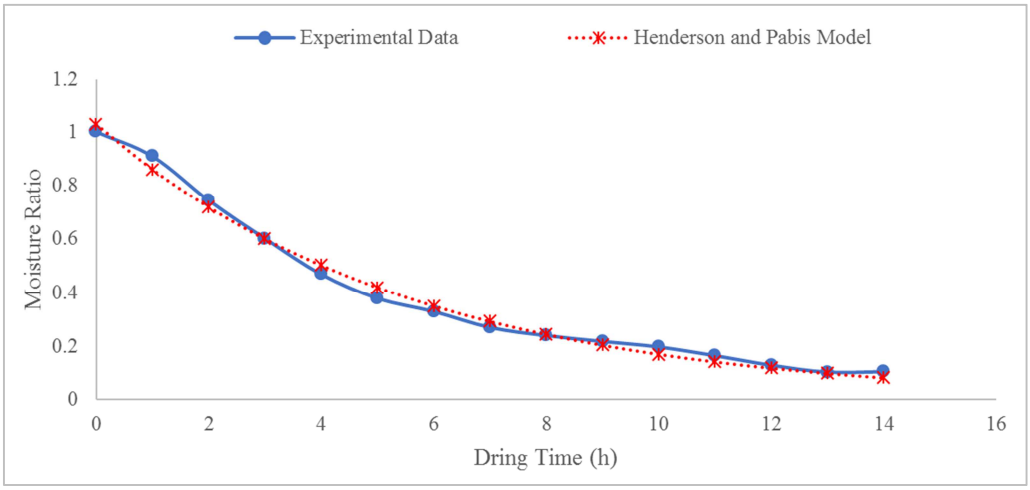

Figure 34. *Henderson and Pabis model fitting to experimental data in exhaust gas mode of drying.*

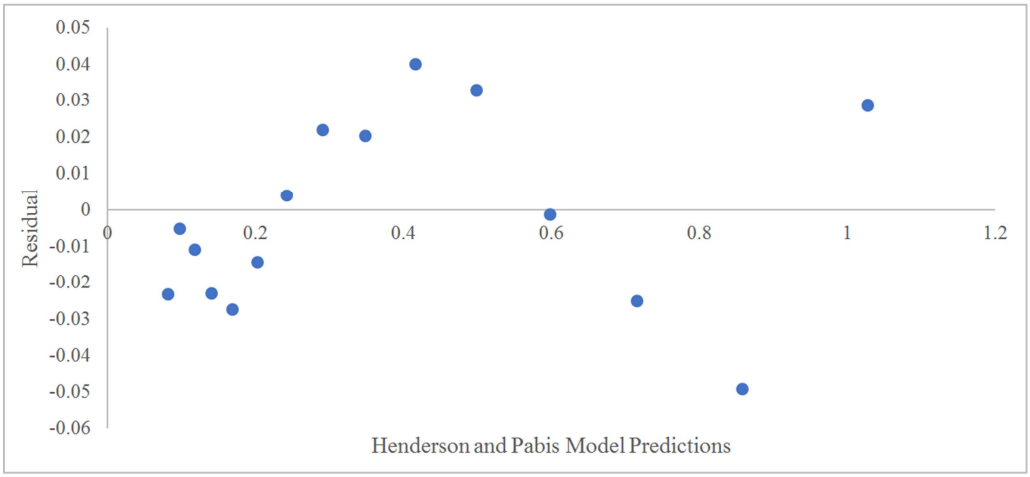

Figure 35. *Henderson and Pabis model predictions and residual plots in exhaust gas mode of drying.*

4. Conclusions

The performance of the solar-exhaust gas greenhouse dryer improved when heat energy from a diesel engine generated exhaust gas was used as a supplement in the drying technique and as a result the drying time for black nightshade seeds was significantly reduced from 11 hours in solar mode to 10 hours in solar-exhaust gas mode of drying. Generally, the drying rate of black nightshade seeds increased with increase in temperature—as observed in solar-exhaust gas drying mode—and decreased with increase in relative humidity—as depicted in exhaust gas drying mode whose experiments were performed between 5:00 p.m. and 7:00 a.m. when solar

radiation was low, and humidity inside the dryer was high due to the presence of water vapour evaporating from the open cooling system of a diesel engine. It may be concluded that thin layer modeling approach is an essential tool in estimating the drying kinetics and describing the drying behaviour of black nightshade seeds from experimental data. Use of RMSE to measure the performance of the models' for numerical predictions of moisture ratio led to the conclusion that Page model with the lowest RMSE value was the most appropriate in describing the drying kinetics of the seeds when the dryer was operated on solar mode. The Logarithmic model had the lowest value of RMSE in both solar-exhaust gas and exhaust gas modes of drying. Accordingly, the Logarithmic model was selected to best characterize thin layer drying of the seeds in the two modes. The average hourly rise in temperature inside the dryer was 8.04°C with a minimum rise of 3.7°C and a maximum of 9.41°C when exhaust gas was utilized to provide heat energy. Significantly, data obtained from the results of thin layer modeling can be used in the design of a solar-exhaust gas greenhouse dryer for farmers who produce climate-smart vegetable crops such as black nightshade. The need for further study to establish the modeling approach's suitability in improving the drying process to eventually minimize the total energy requirements is emphasized.

Conflict of Interest and Authorship Conformation Form

1) All authors have participated in conception, design, analysis, and interpretation of the data; drafting the article, revising it critically for important intellectual content; and approval of the final version.
2) This manuscript has not been submitted to, nor is under review at, another journal or other publishing venue.
3) The authors have no affiliation with any organization with a direct or indirect financial interest in the subject matter discussed in the manuscript.

Nomenclature

a	Drying coefficient specific to Henderson and Pabis model
c	Drying coefficient specific to Logarithmic model
Δm	Change in mass (g)
Δt	Change in time (h)
DR	Drying rate (g/g/h)
db	Dry basis
k	Drying constant (h^{-1})
M	Moisture content (% db)
MR	Moisture ratio
M_t	Moisture content (% db) at time t (h)
M_e	Equilibrium moisture content (%)
M_i	Initial moisture content (% db)
m_d	Final mass (g) of dried sample
m_t	Dried mass (g) of sample at time t (h)
m_i	Initial/instantaneous sample mass (g)
m_{i-1}	Sample mass (g) preceding instantaneous sample mass (g)
n	Drying coefficient specific to Page and Logarithmic models
O_i	Observed values
$\hat{O}_i$	Average of observed values
P_i	Predicted values
$\hat{P}_i$	Average of predicted values
t	Drying time (h)
t_i	Instantaneous drying time (h)
t_{i-1}	Drying time (h) preceding instantaneous drying time (h)

Abbreviations and Acronyms

AOAC	Association of Official Analytical Chemists
EMC	Equilibrium Moisture Content
JKUAT	Jomo Kenyatta University of Agriculture and Technology
RMSE	Root Mean Squared Error
RH	Relative Humidity

Acknowledgements

The authors would like to acknowledge the Japan International Cooperation Agency (JICA) through the AFRICA-ai-JAPAN Project Phase II (2022-2023) for the financial support of this work.

References

[1] Edmonds, J. M., & Chweya, J. A. (1997). *Black nightshades: Solanum nigrum L. and related species* (Vol. 15). Bioversity International.

[2] Hong, T. D., Linington, S., & Ellis, R. H. (1996). *Seed storage behavior: a compendium*.

[3] Schippers, R. (1998). Notes on huckleberry, Solanum scabrum and related black nightshade species. *Natural Resource Institute, University of Greenwich. http://www.dfid. gov.uk/r4d/pdf/outputs/R6964a.pdf. Accessed on*, *20/11/2021*.

[4] Kiburi, F. G., Kanali, C. L., Kituu, G. M., Ajwang, P. O., & Ronoh, E. K. (2020a). Performance evaluation and economic feasibility of a solar-biomass hybrid greenhouse dryer for drying banana slices. *Renewable Energy Focus*, *34*, 60-68.

[5] Ronoh, E. K., Ndirangu, S. N., Kiburi, F. G., Kipsang, M. J., & Rutto, E. J. (2020). Evaluation of thin layer drying models for simulating drying kinetics of jackfruit slices in a solar greenhouse dryer. *African Journal of Horticultural Science*, *17*, 31-42.

[6] Chowdhury, M. M. I., Bala, B. K., & Haque, M. A. (2011). Mathematical modelling of thin layer drying of jackfruit leather. *Journal of Food Processing and Preservation*, *35* (6), 797-805.

[7] Hii, C. L., Law, C. L., & Cloke, M. (2009). Modeling using a new thin layer drying model and product quality of cocoa. *Journal of food engineering*, *90* (2), 191-198.

[8] Onwude, D. I., Hashim, N., Janius, R. B., Nawi, N. M., & Abdan, K. (2016). Modeling the thin layer drying of fruits and vegetables: A review. *Comprehensive reviews in food science and food safety*, *15* (3), 599-618.

[9] Chowdhury, N., Ghosh, A., & Chandra, G. (2008). Mosquito larvicidal activities of solanum villosum berry extract against the dengue vector stegomyia aegypti. *BMC Complementary and Alternative Medicine*, *8* (1), 1-8.

[10] Ekhuya, N. A., Wesonga, J. M., & Abukutsa–Onyango, M. O. (2018). Production, processing, and storage techniques of African nightshade (solanum spp.) seeds and their correlations with farmers' characteristics in western Kenya. *African journal of food, agriculture, nutrition, and development*, *18* (2), 13338-13351.

[11] Feldsine, P., Abeyta, C., & Andrews, W. H. (2002). AOAC International methods committee guidelines for validation of qualitative and quantitative food microbiological official methods of analysis. *Journal of AOAC international*, *85* (5), 1187-1200.

[12] Uluko, H., Kanali, C. L., Mailutha, J. T., & Shitanda, D. (2006). A finite element model for the analysis of temperature and moisture distribution in a solar grain dryer. *The Kenya Journal of Mechanical Engineering*, *2* (1), 47-56.

[13] Kaya, A., Aydın, O., & Demirtaş, C. (2007). Drying kinetics of red delicious apple. *Biosystems Engineering*, *96* (4), 517-524.

[14] Abalone, R., Gastón, A., Cassinera, A., & Lara, M. A. (2006). Thin layer drying of amaranth seeds. *Biosystems Engineering*, *93* (2), 179-188.

[15] Goyal, R. K., Kingsly, A. R. P., Manikantan, M. R., & Ilyas, S. M. (2007). Mathematical modelling of thin layer drying kinetics of plum in a tunnel dryer. *Journal of food Engineering*, *79* (1), 176-180.

[16] Jayas, D. S., Cenkowski, S., Pabis, S., & Muir, W. E. (1991). Review of thin layer drying and wetting equations. *Drying technology*, *9* (3), 551-588.

[17] R Core Team (2023). R: A language and Environment for Statistical Computing. R Foundation for Statistical Computing, Vienna, Austria. https://www.R-project.org/.

[18] Pruim, R. J., Kaplan, D. T., & Horton, N. J. (2017). The mosaic package: helping students to 'think with data' using R. *R Journal*, *9* (1), 77.

[19] Kiburi, F. G., Kanali, C. L., Kituu, G. M., Ajwang, P. O., & Ronoh, E. K. (2020b). Quality evaluation of four banana cultivars dried in a greenhouse dryer operated under different energy modes. *African Journal of Horticultural Science*, *17*, 53-66.

[20] Kiburi, F. G., Mutwiwa, U. N., Ronoh, E. K., Chemain, N., & Yegon, H. K. (2017). Evaluating the performance of dehumidified solar dryer in drying of pumpkin slices (Cucurbita pepo). *African Journal of Horticultural Science*, *11*, 72-81.

[21] Ronoh, E. K., Kanali, C. L., Mailutha, J. T. and Shitanda, D. (2012). Evaluation of solar energy dryer systems on drying behaviour and quality attributes of amaranth grains. *International Journal of Energy Science*, *2* (5), 189-194.

[22] Özbek, B., & Dadali, G. (2007). Thin-layer drying characteristics and modelling of mint leaves undergoing microwave treatment. *Journal of Food Engineering*, *83* (4), 541-549.

[23] Olanipekun, B. F., Tunde-Akintunde, T. Y., Oyelade, O. J., Adebisi, M. G., & Adenaya, T. A. (2015). Mathematical modeling of thin-layer pineapple drying. *Journal of food processing and preservation*, *39* (6), 1431-1441.

[24] Oyerinde, A. S. (2016). Modelling of thin layer drying kinetics of tomato (Lycopersicon esculentum Mill) slices under direct sun and air assisted solar dryer. *International Journal of Engineering and Applied Sciences*, *3* (5), 257660.

[25] Da Silva, W. P., e Silva, C. M., Gama, F. J., & Gomes, J. P. (2014). Mathematical models to describe thin-layer drying and to determine drying rate of whole bananas. *Journal of the Saudi Society of Agricultural Sciences*, *13* (1), 67-74.

[26] Tunde-Akintunde, T. Y. (2011). Mathematical modeling of sun and solar drying of chilli pepper. *Renewable energy*, *36* (8), 2139-2145.

[27] Han, J. W., & Keum, D. H. (2011). Thin layer drying characteristics of rapeseed (*Brassica napus* L.). *Journal of Stored Products Research*, *47* (1), 32-38.

[28] Ronoh, E. K., Kanali, C. L., Mailutha, J. T., & Shitanda, D. (2009). Modeling thin layer drying of amaranth seeds under open sun and natural convection solar tent dryer. *Agricultural Engineering International: the CIGR Ejournal. Manuscript* 1420. Vol. XI. November 2009.

[29] Yaldiz, O., Ertekin, C., & Uzun, H. I. (2001). Mathematical modeling of thin layer solar drying of sultana grapes. *Energy*, *26* (5), 457-465.